

Large dip artifacts in 1.5D internal multiple prediction and their mitigation

Kris Innanen and Pan Pan

ABSTRACT

In this short note we point out that large-dip artifacts, noticeable in unfiltered 1.5D internal multiple predictions, can be mitigated by the employment of a k_g -dependent integration-limiting parameter ϵ . The results are largely consistent with those obtainable by post-prediction filtering, but the $\epsilon(k_g)$ approach is preferable, in that it is tied to our interpretation of the origins of the artifacts.

INTRODUCTION

Luo and co-authors in a recent Leading Edge article point out that most technical successes relating to multiple removal have been reported in marine settings (Luo et al., 2011). This is not to say that interference from internal multiples is not a key problem in land seismic data — just that there seem to be fewer success stories to report. Prestack 1D, or 1.5D, implementations of the inverse scattering series attenuation algorithm (Araújo, 1994; Weglein et al., 1997) are currently being developed with land application particularly in mind (Hernandez and Innanen, 2014; Pan et al., 2014; Pan and Innanen, 2014). Amongst potential responses to the special problems of multiple removal on land, refinement of our use of prediction algorithm parameters holds significant promise. In this short note we discuss the role of the integration-limiting parameter ϵ (as initially identified and applied by Coates and Weglein, 1996) within the algorithm, and investigate the possibility that optimum values of ϵ should vary with offset-wavenumber. We show with a simple synthetic that a fixed constant ϵ is responsible for large-dip artifacts in the prediction. These artifacts can be mitigated with post-prediction filtering, but we further demonstrate that a k_g dependent ϵ , in addition to being a more elegant solution based on the origins of the artifacts, produces a cleaner result.

SCHEME

In Figure 1 we show a synthetic shot record (anticipating later results) in order to quickly illustrate the problem. A split-spread shot gather synthesized over a two interface acoustic model is illustrated in Figure 1a, and the raw internal multiple prediction constructed using the optimum fixed ϵ value derived from analysis of the zero-offset trace (Hernandez, 2012) is illustrated in Figure 1b. The artifacts in question are the large-dip linear events intersecting the bottom axis of the prediction at roughly 1000m and 4000m, which correlate with the large-offset arms of the shallowest primary.

The correlation between the artifacts and the primaries in the original data provides a clue as to their origin. The role of ϵ is to limit the ability of the algorithm to classify nearby sub-events as satisfying the “lower-higher-lower” criterion (Weglein et al., 2003). This relationship, applied to *resolvable events* which are combined in the construction of the prediction, gives rise correctly to internal multiple estimates. However, a finite-length

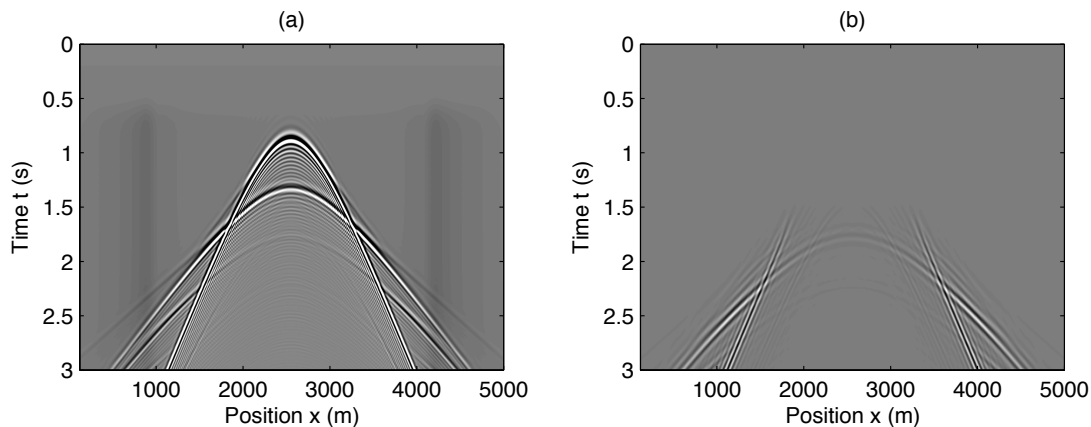


FIG. 1. The issue. (a) Input synthetic data taken over a 2-interface acoustic model; (b) raw prediction generated with fixed ϵ . Large dip artifacts are visible intersecting the bottom of the panel at roughly 1000m and 4000m.

wavelet, internally to itself, has lobes, and the lobes of a single wavelet also obey a lower-higher-lower relationship. If the internal lobes of a wavelet are permitted to act as *bona fide* sub-events, the result is that not just multiples, but primaries are also predicted. In a subsequent subtraction procedure, the artifacts pose a significant threat to primary signal energy.

The fact that the artifacts in Figure 1b both match with primaries, and emerge at large dip, is suggestive that the ϵ value, which was chosen as optimum using an essentially 1D (i.e., lateral wavenumber $k_g = 0$) analysis of the zero-offset trace, is too small in application to the larger k_g values.

Our scheme to manage these artifacts is illustrated in Figure 2. The input to the internal multiple prediction algorithm, $b_1(k_g, z)$, is illustrated schematically in Figure 2a. The left edge of the panel corresponds to $k_g = 0$; a vertical slice through b_1 at this point contains the normal incidence plane wave contribution to the data. In 1D internal multiple prediction, the wavelet duration, which is represented by the blue wedge sliced through at $k_g = 0$, leads to a sensible choice for ϵ (Figure 2b). However, since b_1 varies significantly with k_g it stands to reason this value is not optimal for every vertical slice through b_1 — the discrepancy becomes increasingly apparent moving from left to right in Figure 2b. The variation of $|b_1(k_g, z)|$ is not simple, but it has some basic properties, the main one being an event “spreads out” in depth as k_g grows. Based on this we advocate an ϵ which is a growing function of k_g (Figure 2c).

NUMERICAL EXAMPLE

To illustrate the potential benefits of this scheme, we create a synthetic data set (using the acoustic finite-difference package in the CREWES Matlab toolbox) as follows. A two-interface acoustic model with large impedance contrasts is chosen (Figure 3), and a single split-spread shot record is modelled from it (Figure 4).

Next, we Fourier transform the data, re-sample, and scale, to form the input $b_1(k_g, k_z)$, in which k_z is the Fourier variable conjugate to pseudo-depth $z = c_0 t/2$. This is inverse

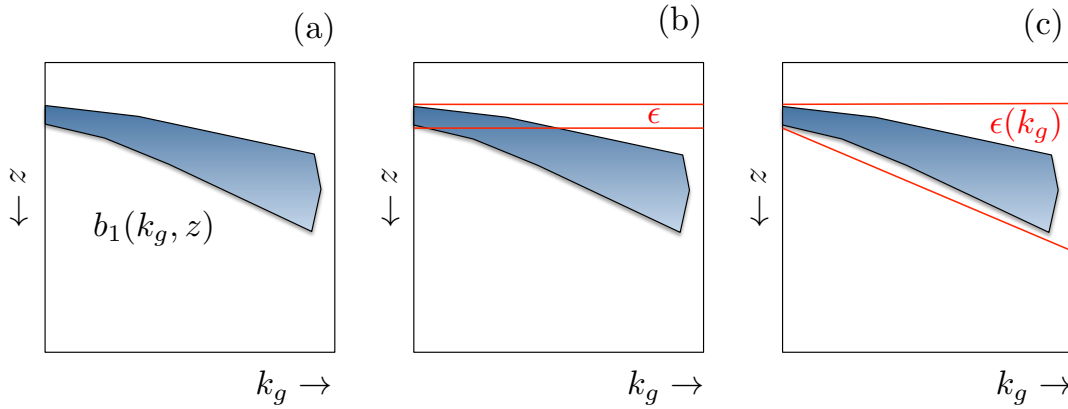


FIG. 2. Artifact mitigation scheme. (a) Schematic illustration of the input $b_1(k_g, z)$ (containing one event) to the prediction algorithm; (b) integration-limiting parameter ϵ fixed at a size appropriate to $k_g = 0$; (c) our proposed response takes the form of $\epsilon(k_g)$ which broadly captures the tendency of $b_1(k_g, z)$ to spread out in z as k_g increases.

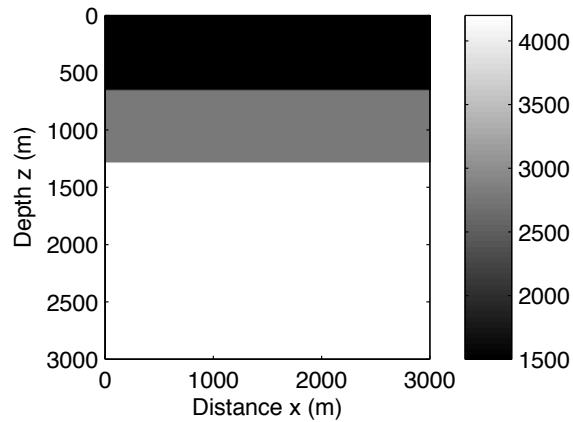


FIG. 3. Acoustic model input to synthetic modelling code. Medium velocities range from 1500m/s (top) to 2800m/s (middle) to 4200m/s (bottom).

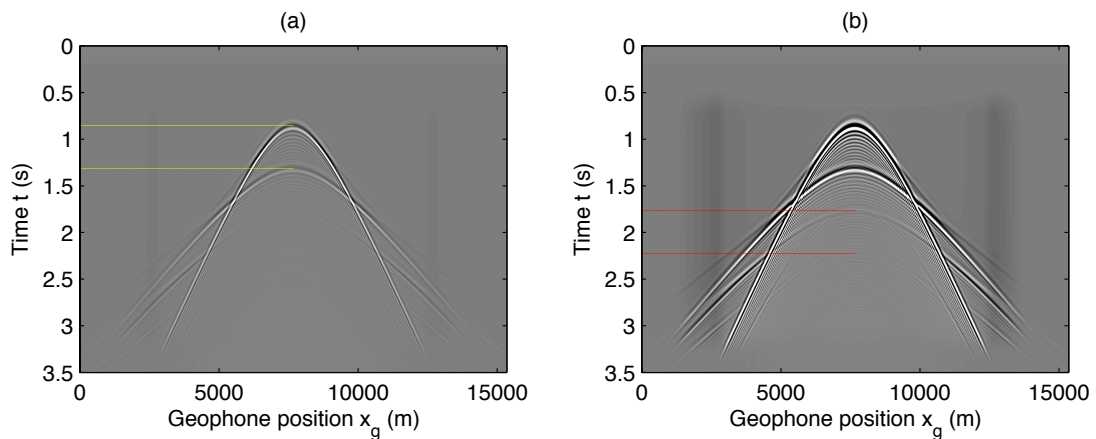


FIG. 4. Synthetic data, large time/offset taper included. (a) Two reflected primaries are indicated with yellow lines; (b) with the clip lowered, two of the series of internal multiples are illustrated with red lines.

Fourier transformed over k_z to obtain the input quantity $b_1(k_g, z)$. The absolute values of $b_1(k_g, z)$ are plotted in Figure 5. On the left edge of the panel ($k_g = 0$) the two primaries can be seen intersecting the z axis at their proper pseudo-depths (i.e., the depths which an assumed velocity of $c_0 = 1500\text{m/s}$ would place them). Their width in the z direction is determined by the velocity and the time-duration of the wavelet. Moving to the right to growing values of k_g , the spreading of $|b_1(k_g, z)|$ in z is notable.

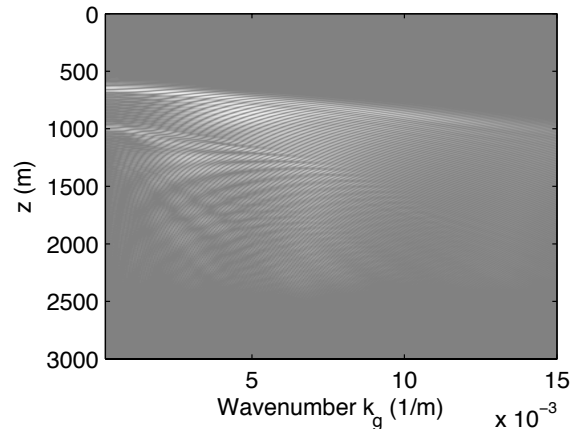


FIG. 5. The input to the internal multiple prediction algorithm $|b_1(k_g, z)|$.

The input is then fed raw into the CREWES Matlab implementation of the internal multiple prediction algorithm with ϵ initially fixed in units of time to 0.3s, which keeps the multiples (as analyzed in the zero-offset trace) separate, while accommodating the ringing wavelet that arises in the 2D acoustic modelling. The input data and the resulting prediction are illustrated in Figures 6a and b, which we discussed in the previous section.

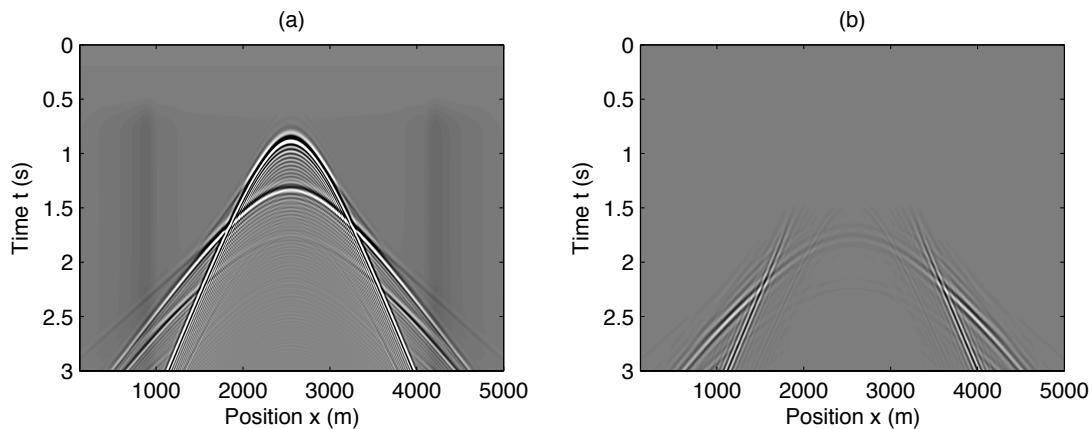


FIG. 6. (a) Input synthetic data, and (b) prediction with fixed ϵ optimized by analyzing the zero-offset trace. The artifacts discussed in the previous section are again visible.

Because the artifacts have a characteristically large dip, not shared by the multiples in the prediction, we can of course mitigate this problem by filtering out the offending k_g values, post-prediction. This is illustrated in Figure 7.

However, a cleaner result that keeps us tied to the actual origins of the artifacts is obtainable with a relatively simple extension of the internal multiple prediction to incorporate

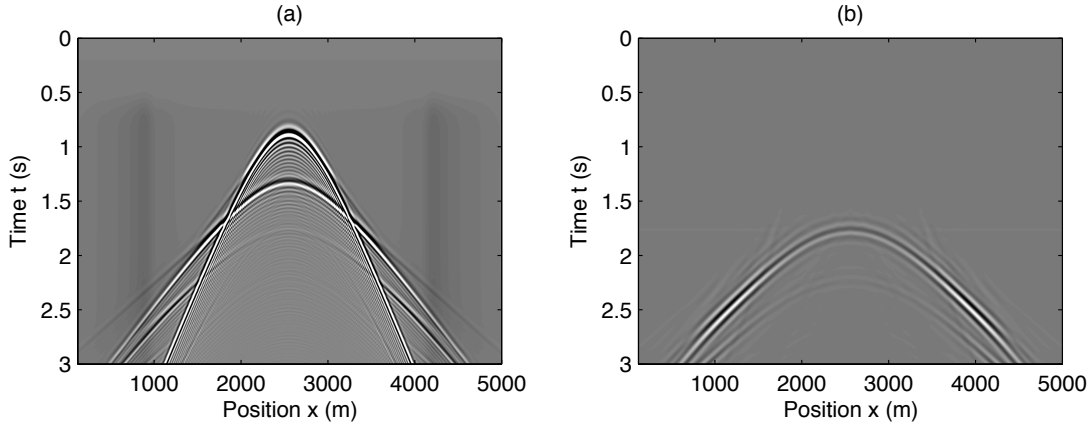


FIG. 7. Artifact mitigation can be accomplished by filtering the spurious dips after the prediction is complete.

a varying $\epsilon(k_g)$. A linear ϵ which interpolates between a minimum (1D or $k_g = 0$) value ϵ_{\min} , and a maximum value ϵ_{\max} to be in place at $k_g = k_{g\max}$, the rightmost edge of the panel in Figure 5, is chosen:

$$\epsilon(k_g) = \left(\frac{\epsilon_{\max} - \epsilon_{\min}}{k_{g\max}} \right) k_g + \epsilon_{\min}. \quad (1)$$

In Figure 8, the result of this prediction is plotted, generated using parameters

$$\begin{aligned} \epsilon_{\max} &= 2s \\ \epsilon_{\min} &= 0.3s. \end{aligned} \quad (2)$$

That is, the integration limits apply, essentially, a full stoppage of prediction by the time k_g reaches a maximum, while matching the originally-determined optimum value at $k_g = 0$ (i.e., the 1D end-member). It achieves by-and-large the same result as the post-hoc filtering, but perhaps a little more cleanly, and in a manner which directly addresses the problem at its root.

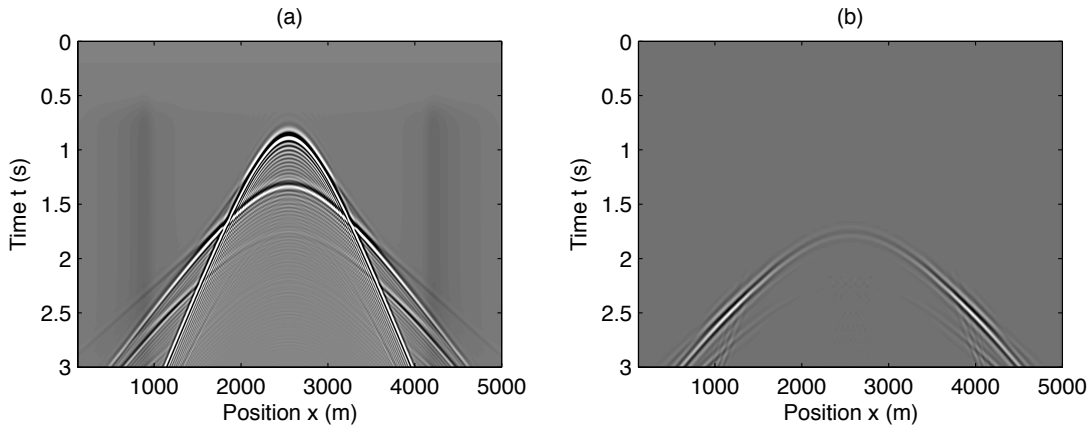


FIG. 8. Prediction constructed using a linear $\epsilon(k_g)$.

CONCLUSIONS

We point out that large-dip artifacts noticeable in unfiltered 1.5D internal multiple predictions can be mitigated by the employment of a k_g -dependent integration-limiting parameter ϵ . The results are largely consistent with those obtainable by post-prediction filtering, but the $\epsilon(k_g)$ approach is preferable in that it is tied to our interpretation of the origins of the artifacts.

One potential benefit of adopting this approach to mitigation is that, in full 2D or even 3D versions of the algorithm, more complex artifacts, originating similarly, may arise, which simple post-hoc filtering cannot adequately fix, but which sub-event management via, for instance, $\epsilon(k_g, k_s)$, can. This is of course only a speculative statement at the moment.

ACKNOWLEDGEMENTS

We thank the sponsors of CREWES for continued support. This work was funded by CREWES and NSERC (Natural Science and Engineering Research Council of Canada) through the grant CRDPJ 379744-08.

REFERENCES

- Araújo, F. V., 1994, Linear and non-linear methods derived from scattering theory: backscattered tomography and internal multiple attenuation: Ph.D. thesis, Universidade Federal da Bahia.
- Coates, R. T., and Weglein, A. B., 1996, Internal multiple attenuation using inverse scattering: results from prestack 1 & 2d acoustic and elastic synthetics: SEG Technical Program Expanded Abstracts, 1522–1525.
- Hernandez, M. J., 2012, Internal multiple prediction: an application on synthetic data, physical modelling and field data: M.Sc. thesis, University of Calgary.
- Hernandez, M. J., and Innanen, K. A., 2014, Identifying internal multiples using 1d prediction: physical modelling and land data examples: Canadian Journal of Geophysical Exploration, **39**, No. 1, 37–47.
- Luo, Y., Kelamis, P. G., Fu, Q., Huo, S., Sindi, G., Hsu, S., and Weglein, A. B., 2011, Elimination of land internal multiples based on the inverse scattering series: The Leading Edge, **30**, No. 8, 884–889.
- Pan, P., and Innanen, K. A., 2014, Internal multiple prediction on Hussar synthetics: CREWES Annual Report, **26**.
- Pan, P., Innanen, K. A., and Wong, J., 2014, 1.5D internal multiple prediction on physical modelling data: CREWES Annual Report, **26**.
- Weglein, A. B., Araújo, F. V., Carvalho, P. M., Stolt, R. H., Matson, K. H., Coates, R. T., Corrigan, D., Foster, D. J., Shaw, S. A., and Zhang, H., 2003, Inverse scattering series and seismic exploration: Inverse Problems, , No. 19, R27–R83.
- Weglein, A. B., Gasparotto, F. A., Carvalho, P. M., and Stolt, R. H., 1997, An inverse-scattering series method for attenuating multiples in seismic reflection data: Geophysics, **62**, No. 6, 1975–1989.